Available online at www.sciencedirect.com
SCIENCE DIRECT®
ELSEVIER
Physica D 178 (2003) 127–148
PHYSICA D
www.elsevier.com/locate/physd

Coarsening dynamics of the convective Cahn-Hilliard equation

Stephen J. Watson [a,*], Felix Otto [b], Boris Y. Rubinstein [a], Stephen H. Davis [a]

[a] *Engineering Sciences and Applied Mathematics, McCornick School of Engineering and Applied Science, Northwestern University, 2145 Sheridan Road, Evanston, IL 60208, USA*
[b] *Institut für Angewandte Mathematik, Universität Bonn, Wegelstraße 10, Zimmer 256, 53115 Bonn, Germany*

Received 13 March 2002; received in revised form 12 December 2002; accepted 24 January 2003
Communicated by R.P. Behringer

Abstract

We characterize the coarsening dynamics associated with a convective Cahn-Hilliard equation (cCH) in one space dimension. First, we derive a sharp-interface theory through a matched asymptotic analysis. Two types of phase boundaries (kink and anti-kink) arise, due to the presence of convection, and their motions are governed to leading order by a nearest-neighbors interaction coarsening dynamical system ($\mathcal{CDS}$). Theoretical predictions on $\mathcal{CDS}$ include:

- The characteristic length $\mathcal{L}_{\mathcal{M}}$ for coarsening exhibits the temporal power law scaling $t^{1/2}$; provided $\mathcal{L}_{\mathcal{M}}$ is appropriately small with respect to the *Peclet* length scale $\mathcal{L}_{\mathcal{P}}$.
- Binary coalescence of phase boundaries is impossible.
- Ternary coalescence only occurs through the *kink-ternary* interaction; two kinks meet an anti-kink resulting in a kink.

Direct numerical simulations performed on both $\mathcal{CDS}$ and cCH confirm each of these predictions. A linear stability analysis of $\mathcal{CDS}$ identifies a *pinching* mechanism as the dominant instability, which in turn leads to kink-ternaries. We propose a self-similar period-doubling *pinch ansatz* as a model for the coarsening process, from which an analytical coarsening law for the characteristic length scale $\mathcal{L}_{\mathcal{M}}$ emerges. It predicts both the scaling constant c of the $t^{1/2}$ regime, i.e. $\mathcal{L}_{\mathcal{M}} = ct^{1/2}$, as well as the crossover to logarithmically slow coarsening as $\mathcal{L}_{\mathcal{M}}$ crosses $\mathcal{L}_{\mathcal{P}}$. Our analytical coarsening law stands in good qualitative agreement with large-scale numerical simulations that have been performed on cCH.

PACS: 05.45.−a; 68.35.Ja; 81.10.Aj

Keywords: Driven phase ordering; Coarsening dynamical system; Scaling laws

1. Introduction

The kinetics of *driven* phase-ordering systems offers new and rich possibilities in phenomenology. To model a driven system one must identify both the energetics and the dynamics of phase boundaries, in distinction with equilibrium phase separation [1], where energetics alone suffices. A paradigm of this distinction arises in the first-order phase transformation of a melt in contact with its solid. Here, sufficient undercooling of the melt breaks

* Corresponding author. Fax: +1-847-491-4398.
E-mail address: s-watson@northwestern.edu (S.J. Watson).

0167-2789/03/$ – see front matter © 2003 Elsevier Science B.V. All rights reserved.
doi:10.1016/S0167-2789(03)00048-4

thermodynamic equilibrium at the interface and then a dynamic condition expressing the systems response is also required; e.g. the Gibbs-Thomson condition with *kinetic undercooling*.

The Cahn-Hilliard equation (CH) governs the *spinodal decomposition* of binary alloys under isothermal conditions [2], in one space dimension:

$$q_t = [\mathcal{W}'(q) - \varepsilon^2 q_{xx}]_{xx}, \tag{1}$$

where $q(x,t)$ is the *phase fraction* (order parameter) at the spatial location x at time t, $\mathcal{W}(q)$ a symmetric *double well* with minima at $q = \pm 1$, and ε a dimensionless *interfacial width*. The coarsening dynamics of CH serves as an archetypal example of an equilibrium phase separation process. Here, an initially spatially homogeneous mixture, $q \equiv 0$, is driven to segregate by a uniform reduction in temperature (*quenching*). A fine-grained phase mixture is initially formed, and this morphology subsequently coarsens into larger-scale structures with a characteristic length scale $\mathcal{L}(t)$. Among the properties of the CH theory are the phase selection rule for the mixture through a bi-tangent construction on $W(q)$ [3], and the logarithmically slow coarsening rate in one space dimension [4]:

$$\mathcal{L}(t) \sim \ln t.$$

The process of *thermal faceting*, in which a planar crystalline surface breaks up into hill (anti-kink) and valley (kink) structures following a change in temperature, is analogous to spinodal decomposition. In particular, the faceting of a thermodynamically unstable planar surface which *relaxes* without net growth (*anneals*) has also been modeled with equations of CH type [5,6]; the analogy is exact in 1D situations, but important distinctions arise in higher dimensions [7]. Here, the orientation of the local tangent plane serves as a (vector) order parameter and the surface tension induces an effective free energy. Furthermore, the surface tension is sufficiently anisotropic that certain crystal surfaces are thermodynamically unstable and hence missing in the crystal equilibrium state (Wulff shape [8]). A stable pair of facets corresponds to bi-tangent points of the surface free energy, and the hill-valley structures coarsen with a rate depending on the mechanism of surface relaxation [9], the effective dimensions of the structure, and also the symmetry group of the crystal surface [7,10].

When thermal faceting of a crystal surface involves net *growth* into its melt (or vapor), then convective terms augment the CH structure [9,11,12]; roughly, the net growth of facets in their normal direction convects the order parameter. Now provided the strength of convection is small enough, spinodal decomposition reminiscent of CH again arises. However, the coarsening rates that have been observed numerically are significantly faster than the non-growth counterparts; e.g. one regime of the 1D convective Cahn-Hilliard equation gives [11,13]:

$$\mathcal{L}(t) \sim t^{1/2}.$$

Remark 1. Large-enough growth rates may arrest coarsening or even induce spatio-temporal chaos of the crystal surface [14].

In this paper, we study the coarsening dynamics of a convective Cahn-Hilliard equation (cCH) in one space dimension, in dimensionless form:

$$q_t - qq_x = (q^3 - q - \varepsilon^2 q_{xx})_{xx}. \tag{2}$$

Leung [15] proposed it as a continuum description of phase separation of a *lattice gas driven* by an applied field. In a similar spirit, Emmot and Bray [13] proposed it as a model for spinodal decomposition of a binary alloy in an external field. In both cases, an assumed order parameter dependence of the *mobility* couples to the external field, thereby inducing the Burgers convection term.

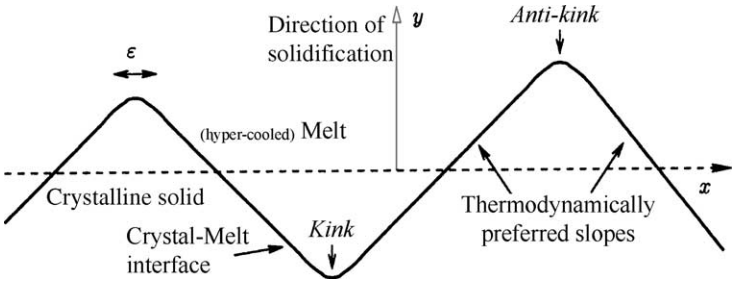

Fig. 1. Schematic representation of a faceted 2D crystal growing into its (hypercooled) melt. The local slope q of the crystal–melt interface is measured relative to a frame of reference $x - y$ co-moving with the direction of solidification. The rounded corners between facets have width $O(\varepsilon)$, and the hill and valley corners are denoted as *kinks* and *anti-kinks*, respectively.

Golovin et al. [11] derived (2) as a model for kinetically controlled growth of two-dimensional crystals; see also Smilauer et al. [12] for a closely related model arising in epitaxial growth. Watson [16] has subsequently identified (2) as a *small slope* approximation to the geometric crystal-growth model derived by Gurtin et al. [19,20]; their geometric model takes the form of a *a driven anisotropic Willmore flow*[1]. In the small slope setting, q denotes the slope (phase) of the crystal surface, and ε a non-dimensional width of the high curvature corners (*phase boundaries*); see Fig. 1. The broken up-down symmetry due to crystal growth is captured by the Burgers convection, qq_x, which breaks the symmetry $x \to -x$ in (2). In turn, the valley corner (*kink*) and hill corner (*anti-kink*) are not symmetrically related. In addition, the *bi-tangent* construction for the identification of the slopes (phases) far from the hill and valley corners is broken; valley slopes are steeper than the expected $q = \pm 1$, while hill slopes are shallower [11,13,15]. The failure of this thermodynamic construction marks cCH as a *driven* phase-ordering system.

We perform a matched asymptotic analysis of cCH, Eq. (2), as $\varepsilon \to 0^+$, that leads to a sharp-interface theory of kink/anti-kink interaction [17,18]. It shows that the asymmetry between a kink and anti-kink induces a convective–diffusive flux of the order parameter between them. This is turn drives these discontinuities in a manner given by the Rankine-Hugoniot relation; recall that q is a conserved quantity. The result is a nearest-neighbor interaction dynamical system for the kink/anti-kink locations. Our theory generalizes that of Emmot and Bray [13], which is valid only for dimensionless length scales $\varepsilon \ll \mathcal{L} \ll 1$, to all length scales $\varepsilon \ll \mathcal{L}$.

The average separation (*morphological length scale*) $\mathcal{L}_{\mathcal{M}}$ between successive phase boundaries grows in time as coalescing kinks and anti-kinks annihilate one another. We develop a theory for this *coarsening dynamical system* ($\mathcal{CDS}$) which rigorously establishes

(i) The characteristic length $\mathcal{L}_{\mathcal{M}}$ exhibits the temporal scaling $t^{1/2}$, provided $\mathcal{L}_{\mathcal{M}}$ is appropriately small with respect to the *Peclet* length scale $\mathcal{L}_{\mathcal{P}}$.
(ii) Binary coalescence of phase boundaries is impossible.
(iii) Ternary coalescence of phase boundaries may only occur through a *kink-ternary*; two kinks meet an anti-kink resulting in a kink.

The unusual coarsening mechanisms described in (ii) and (iii) are novel, and stand in marked contrast with the coarsening dynamics of the CH, Eq. (1), where binary coalescence of phase boundaries is generic [4,22,23]. We present direct numerical simulations of cCH which confirm (ii) and (iii). Further, our predicted coarsening law (i) coincides with the direct numerical simulations of cCH [14].

[1] The Willmore flow arises in differential geometry [21].

A linear stability analysis of a spatially periodic kink/anti-kink array identifies *pinching* as the dominant instability; pairs of kinks move towards the intervening anti-kink. We note also that the "opposite" maneuver, whereby two anti-kinks move pairwise towards the intervening kink, is the most stable disturbance. Both these results follow directly from the spectral properties of a new class of matrices, *alternating circulant matrices* [24], which are related to circulant matrices [25]. Following the pinch instability into the nonlinear regime yields, via kink-ternary coalescence, a periodic array of twice the initial separation.

We propose a self-similar (spatial-) period-doubling *pinching* ansatz as a description of the coarsening process. It involves application of a scale-invariant initial disturbances on spatially periodic arrays of kink/anti-kinks in the *pinch direction*; i.e. the dominant linear-instability eigenvector. As noted, this results in an array of twice the initial period, upon which we iterate the procedure. Our motivation for the ansatz is twofold. First, the non-existence of ternary coalescence involving two anti-kinks and a kink (see (iii)) is a reflection of the repulsive interaction between anti-kinks. We assume that this repulsion enforces a "near-periodicity" of anti-kinks during throughout the evolution, which in turn highlights the relevance of the *pinch instability*. Second, we recall the self-similarity of the length scale distribution observed by [13] (valid even for "early times"), and note also that our simulations qualitatively display marked "self-similarity" in the *coarsening path*. The scale-invariant disturbance component of our ansatz is intended to capture the scale-invariant deviations of the full system from periodicity.

An analytical coarsening law for cCH is derived from our pinch ansatz for $\mathcal{CDS}$, which is valid over all morphological length scales $\mathcal{L}_{\mathcal{M}} \gg \varepsilon$. It qualitatively captures all the essential features of the numerically calculated coarsening law [14]. In particular, it identifies the crossover to logarithmically slow coarsening to occur when $\mathcal{L}_{\mathcal{M}} \sim \mathcal{L}_{\mathcal{P}}$, thereby clarifying this numerically observed transition. Furthermore, since we have specified the *coarsening path*, we are also able to identify the scaling constant c of the $t^{1/2}$ regime; namely,

$$\mathcal{L}_{\mathcal{M}} = \frac{\sqrt{3}}{\sqrt[4]{2}(\eta^2 - 2\ln\eta - 1)^{1/2}}\varepsilon^{1/2}t^{1/2}, \quad \varepsilon \ll \mathcal{L}_{\mathcal{M}} \ll 1,$$

where $0 < \eta \ll 1$ is the scale-invariant disturbance parameter of our period-doubling coarsening ansatz.

2. The convective Cahn-Hilliard equation

We consider the following one-dimensional convective Cahn-Hilliard equation (cCH):

$$q_{\bar{t}} - Vqq_{\bar{x}} = \mu(q^3 - q - \nu^2 q_{\bar{x}\bar{x}})_{\bar{x}\bar{x}}, \tag{3}$$

where the dimensionless order parameter $q(\bar{x}, \bar{t})$ is a function of dimensional space $\bar{x} \in \mathbb{R}$ and time $\bar{t}$, V a speed ($[V] = LT^{-1}$), μ a mobility ($[\mu] = L^2T^{-1}$) and ν a microscopic length scale ($[\nu] = L$). Eq. (3) serves, e.g. as a phenomenological model of faceting in kinetically controlled crystal growth [11,16].

2.1. Scaling analysis

The convection balancing diffusion supplies the *Peclet* length scale $\mathcal{L}_{\mathcal{P}}$ and associated time scale $t_{\mathcal{P}}$ given by

$$\mathcal{L}_{\mathcal{P}} := \frac{\mu}{V}, \qquad t_{\mathcal{P}} := \frac{\mu}{V^2}.$$

We now re-scale (3) through

$$x = \frac{\bar{x}}{\mathcal{L}_{\mathcal{P}}}, \quad \text{and} \quad t = \frac{\bar{t}}{t_{\mathcal{P}}} \tag{4}$$

and arrive at the dimensionless form of cCH:

$$q_t - qq_x = (q^3 - q - \varepsilon^2 q_{xx})_{xx}, \tag{5}$$

where $\varepsilon := \nu/\mathcal{L}_P$.

Throughout the remainder of the paper, all length and time scales will be in the dimensionless form associated with the scaling (4), unless otherwise stated.

2.2. Previous coarsening studies

Numerical simulations of cCH, Eq. (5), have been previously carried out in [13,14] in the regime[2] $\varepsilon \ll 1$. We now summarize the pertinent observations from these simulation studies. First, the spatially homogeneous state $q = 0$ is unstable and upon disturbance develops a periodic structure with a wavelength λ consistent with that predicted by a linear stability analysis; namely, $\lambda = 2\sqrt{2}\pi\varepsilon$. The "wavelength" of the solution then increases until a well-defined interfacial structure is apparent; then there are "extended" regions where $q \simeq \pm 1$, connected through rapid transition layers (*phase boundaries*) of width $O(\varepsilon)$. Looking in the direction of increasing x, the "step up" transition phase boundary, where $q = -1 \to q = 1$, is referred to as a *kink*, while the step down layer, where $(q = 1 \to q = -1)$ is an *anti-kink*; see Fig. 3.

The average separation (*morphological length scale*) $\mathcal{L}_\mathcal{M}$ between successive phase boundaries continues to grow in time through kink/anti-kink coalescence and their subsequent mutual annihilation. Three distinct regimes in the scaling behavior of (the dimensionless) $\mathcal{L}_\mathcal{M}(t)$ may be discerned in the numerical studies of (5) appearing in [13,14]. They are summarized in the following table:

Scaling regime	Scaling law for $\mathcal{L}_\mathcal{M}(t)$
$\varepsilon \ll \mathcal{L}_\mathcal{M} \ll 1$	$t^{1/2}$
$\mathcal{L}_\mathcal{M} \simeq 1$	*Crossover*
$\mathcal{L}_\mathcal{M} \gg 1$	$\ln t$

Recalling (4), one sees that *crossover* scaling emerges when the morphological length scale $\mathcal{L}_\mathcal{M}(t)$ is comparable to the Peclet length scale $\mathcal{L}_\mathcal{P}$.

Remark 2. When $\varepsilon \sim 1$, the morphologies of solutions do not coarsen in time but rather display periodic patterns, while for $\varepsilon \gg 1$ solutions become *rough* [14]. This is related to the fact that formally the cCH approaches the Kuramoto-Sivashinsky equation (KS) as $\varepsilon \to \infty$, and solutions of KS are known to display spatio-temporal chaos.

We now proceed to develop a sharp-interface theory for cCH from which we may deduce all of the above scaling behavior.

3. Sharp-interface theory

The governing equation (5) is singularly perturbed in the limit $\varepsilon \to 0^+$, with $\partial/\partial x = O(1)$. In this section, we discuss the associated matched asymptotic expansions. Since the parameter ε sets a length scale for transitions, we shall see that the associated outer problem yields a sharp-interface theory.

[2] See Remark 2.

3.1. Matched asymptotic analysis as $\varepsilon \to 0^+$

We refer to (5) as the outer equation, since $\varepsilon \to 0^+$ with $\partial/\partial x$ fixed yields a singular perturbation. The inner equation arises from re-scaling to the inner dimensionless length scale ε. Since the kinks and anti-kinks are in general moving, we need to select an inner coordinate with respect to a moving frame. So, for the kink at $x = k(t;\varepsilon)$, we take the inner coordinate X to be

$$X = \frac{x - k(t;\varepsilon)}{\varepsilon}$$

and re-write (5) in terms of the inner solution $Q(X,t) = q(x,t)$ as

$$\varepsilon^2 Q_t - \varepsilon \dot{k} Q_X - \varepsilon Q Q_X = (Q^3 - Q - Q_{XX})_{XX}, \tag{6}$$

similarly for the anti-kink $a(t)$.

Remark 3. We give a complete matched asymptotic analysis through order $O(\varepsilon)$ in Appendix A. Therein, we establish that the kink velocity $\dot{k}(t)$ is of order $O(\varepsilon)$, consistent with the fact that $\varepsilon = 0$ corresponds to stationary solutions.

Since the kink and anti-kink velocities are of order $O(\varepsilon)$ (see (A.9), (A.14) and (A.15)), it follows that (6) is asymptotically equivalent through order $O(\varepsilon)$ with the time-independent equation:

$$-\varepsilon Q Q_X = (Q^3 - Q - Q_{XX})_{XX}. \tag{7}$$

Now (7) has two exact solutions $\mathcal{K}(X)$ and $\mathcal{A}(X)$, identified in [15], given by

$$\mathcal{K}(X) := \left(1 + \frac{\varepsilon}{\sqrt{2}}\right)^{1/2} \tanh\left[\left(1 + \frac{\varepsilon}{\sqrt{2}}\right)^{1/2} X\right] \quad \text{(kink)} \tag{8}$$

and

$$\mathcal{A}(X) := -\left(1 - \frac{\varepsilon}{\sqrt{2}}\right)^{1/2} \tanh\left[\left(1 - \frac{\varepsilon}{\sqrt{2}}\right)^{1/2} X\right] \quad \text{(anti-kink)}. \tag{9}$$

Remark 4. There is a family of stationary profiles associated with the transition from positive to negative values of q (kinks), while the anti-kink profile (9) is the unique profile connecting negative to positive values of q; see [13,16]. However, the matching condition between the *inner* and *outer problems* is independent of the choice of inner kink solution [16]. For simplicity, we use the particular kink given by (8) in our analysis.

We note here that the asymptotic values as $X \to \infty$ of $\mathcal{K}(X)$ and $\mathcal{A}(X)$ are

$$\lim_{X\to\pm\infty} \mathcal{K}(X) = \pm\left(1 + \frac{\varepsilon}{\sqrt{2}}\right)^{1/2}, \qquad \lim_{X\to\pm\infty} \mathcal{A}(X) = \mp\left(1 - \frac{\varepsilon}{\sqrt{2}}\right)^{1/2}. \tag{10}$$

We see that the presence of convection ($\varepsilon \neq 0$) introduces a fundamental asymmetry between kinks and anti-kinks, which is not present in the Cahn-Hilliard theory ($\varepsilon = 0$). In particular, the bi-tangent construction [3] for identifying "co-existent phases" is destroyed, as evidenced by (10) [11,13,15]. On a deeper level, this is a reflection of the non-equilibrium nature of the underlying phase-transformation process when convection is present.

We now match these inner solutions to the outer solution, which we represent in the form:

$$q(x,t) = q_0(x,t) + q_1(x,t)\varepsilon + \mathrm{O}(\varepsilon^2).$$

It follows from the matched asymptotic analysis presented in Appendix A that the combined approximation $q^{\mathrm{c}} := q_0 + q_1\varepsilon$ is equivalent through order $\mathrm{O}(\varepsilon)$ with the conservation law

$$q^{\mathrm{c}}_t + J_x = 0 \quad \text{for} \quad (x,t) \in \mathbb{R} \times [0,\infty) \tag{11}$$

with flux J given by

$$J = \begin{cases} -q^{\mathrm{c}} - 2q^{\mathrm{c}}_x, & x \in (k(t), a(t)), \\ q^{\mathrm{c}} - 2q^{\mathrm{c}}_x, & x \in (a(t), k(t)), \end{cases} \tag{12}$$

and subject to the Dirichlet boundary conditions:

$$\begin{aligned} &q^{\mathrm{c}}(k(t)^-) = -1 - \frac{1}{2\sqrt{2}}\varepsilon, \qquad q^{\mathrm{c}}(k(t)^+) = 1 + \frac{1}{2\sqrt{2}}\varepsilon, \qquad q^{\mathrm{c}}(a(t)^-) = 1 - \frac{1}{2\sqrt{2}}\varepsilon, \\ &q^{\mathrm{c}}(a(t)^+) = -1 + \frac{1}{2\sqrt{2}}\varepsilon, \end{aligned} \tag{13}$$

where $q^{\mathrm{c}}(k(t)^-)$ and $q^{\mathrm{c}}(k(t)^+)$ denote the limiting values of q^{c} as the kink location $k(t)$ is approached from the left and the right, respectively; similarly for the anti-kinks.

It follows from the conservation law (11) that the speed of the kink $\dot{k}(t)$ (k-shock) is given by the Rankine-Hugoniot relation:

$$\dot{k}(t)[q]_{k(t)} = [J]_{k(t)}, \tag{14}$$

where $[J]_{k(t)}$ and $[q]_{k(t)}$ denote, respectively, the jump in the flux J and the order parameter q across the kink at $x = k(t)$; similarly for the anti-kink.

Since the kink and anti-kink velocities are order $\mathrm{O}(\varepsilon)$, it follows that (11) is equivalent through order $\mathrm{O}(\varepsilon)$ with the quasi-static condition:

$$J_x = 0. \tag{15}$$

Utilizing the notation of Fig. 2, the function q^{c} can now be computed from (12), (13) and (15) yielding

$$q^{\mathrm{c}}(x) = \begin{cases} -1 - \dfrac{\varepsilon}{2\sqrt{2}} + \dfrac{\varepsilon}{\sqrt{2}} \dfrac{1 - \exp((x - a_{\mathrm{l}}(t) - L^-)/2)}{1 - \exp(-L^-/2)}, & a_{\mathrm{l}}(t) \le x \le k(t), \\ 1 + \dfrac{\varepsilon}{2\sqrt{2}} - \dfrac{\varepsilon}{\sqrt{2}} \dfrac{1 - \exp((k(t) - x)/2)}{1 - \exp(-L^+/2)}, & k(t) \le x \le a_{\mathrm{r}}(t). \end{cases} \tag{16}$$

A summary of the outer problem (through $\mathrm{O}(\varepsilon)$) is shown in Fig. 2.

Inserting (16) into (12), we find that the flux J between a neighboring kink k and anti-kink a is, through order $\mathrm{O}(\varepsilon)$, given by

$$J = -1 + \frac{\varepsilon}{\sqrt{2}} \frac{1}{\exp(\mathcal{L}/2) - 1}, \tag{17}$$

where $\mathcal{L} = |k(t) - a(t)|$ is the distance between the neighboring kink and anti-kink.

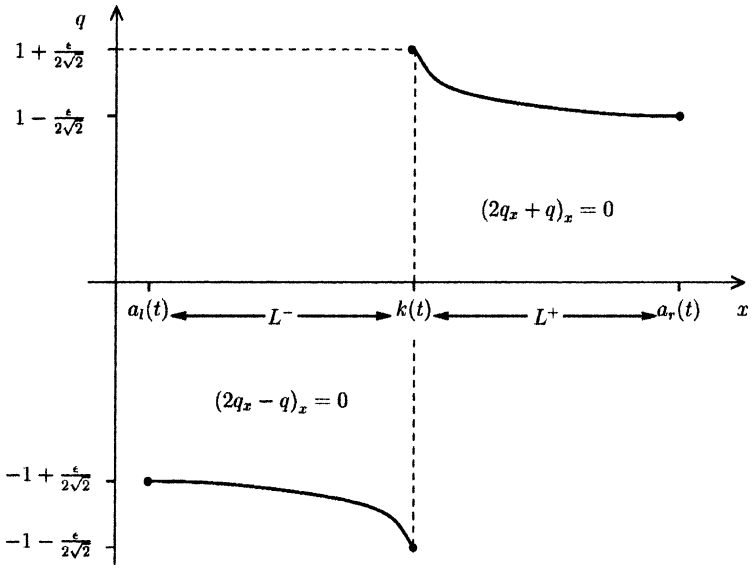

Fig. 2. The sharp-interface limit through O(ε). Here $a_l(t)$ and $a_r(t)$ locate, respectively, the anti-kinks to the left and right of the kink $k(t)$. The two curves are sketches of the outer q profile inserted to guide the eye.

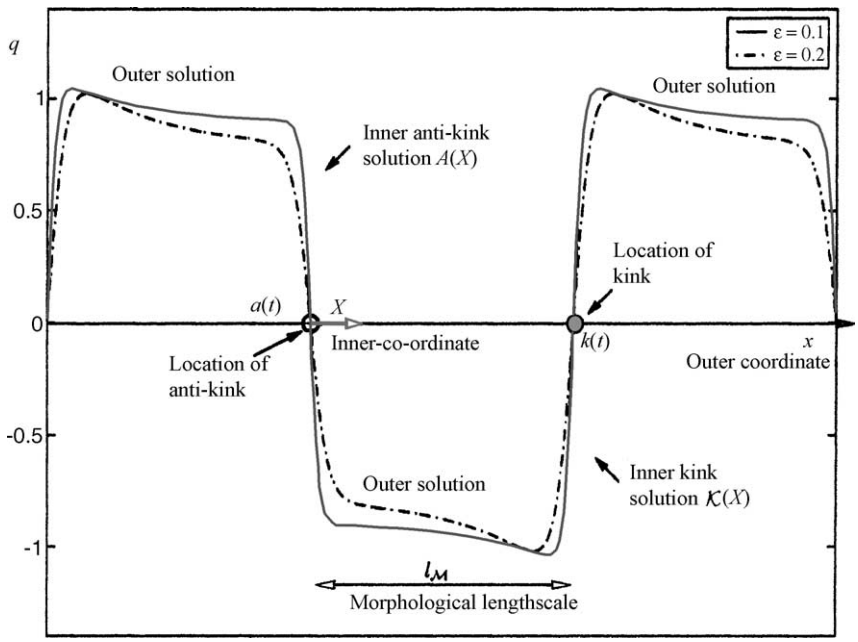

Fig. 3. Structure of the matched asymptotic composite solution of a periodic profile for cCH with wavelength $\lambda = 2\mathcal{L}_{\mathcal{M}}$. Here we have plotted the composite solution for the choice $\mathcal{L}_{\mathcal{M}} = 1$ (i.e. the Peclet length scale) for which diffusion balances convection in the outer regions. Also, ● and ○ denote the location of the kink and anti-kink, respectively.

Remark 5. The O(ε) composite solution, obtained from matching inner and outer solutions, is plotted in Fig. 3 for a choice of parameters associated with the regime $\varepsilon \ll \mathcal{L}_{\mathcal{M}} \simeq 1$. We note that the kink amplitude is suppressed by convection, while the anti-kink amplitude is barely affected. This circumstance is either enhanced or diminished by the respective increase or decrease of the separation between kink and anti-kink.

4. The coarsening dynamical system ($\mathcal{CDS}$)

In this section we show, as a consequence of our sharp-interface theory, that kinks and anti-kinks evolve according to a nearest-neighbor dynamical system. The *coarsening law* of cCH that describes the outcome of a coalescence of kinks and anti-kinks is then identified; the *parity coarsening law*. The $\mathcal{CDS}$ emerges from combining kink/anti-kink dynamics with this *parity coarsening* law. We conclude by showing, through a simple scaling argument, that $\mathcal{CDS}$ obeys the scaling law $\mathcal{L}_{\mathcal{M}} \sim t^{1/2}$, in the regime $\varepsilon \ll \mathcal{L}_{\mathcal{M}} \ll 1$.

We have envisioned the solutions to (3) as an alternating sequence of kinks $\mathcal{K}[X-k(t)]$ and anti-kinks $\mathcal{A}[X-a(t)]$, which are matched through the outer variable x. We make a slight, but convenient abuse of terminology, by now referring to the locations $k(t)$ and $a(t)$ also as kinks and anti-kinks.

4.1. Kink/anti-kink dynamics

Here we identify the dynamical system associated with our sharp-interface theory for kink/anti-kink interaction. As we shall see, kinks and anti-kinks follow different, but "*skew* related", laws of motion. In anticipation of this, we adopt the following useful index convention for these an alternating array of these phase boundaries which takes advantage of this property.

4.1.1. Index convention

Given an alternating array of kink/anti-kink locations on the line, we adopt the (arbitrary) ordering convention of letting kinks have odd indices, which in turn gives anti-kinks even indices.

Let $x_i(t)$ denote the location of the ith phase boundary at time t, and set $L_i(t) := x_{i+1} - x_i$; the distance between the ith and $i+1$th phase boundary (Fig. 4). Recalling (13) and (17), we deduce from the Rankine-Hugoniot relation (14) that through order O(ε):

$$\frac{\mathrm{d}x_i}{\mathrm{d}t} = (-1)^{i+1}[J(L_i) - J(L_{i-1})], \tag{18}$$

where the (effective) *flux function* $J(\mathcal{L})$ is given by

$$J(\mathcal{L}) := \frac{\varepsilon}{2\sqrt{2}} \frac{1}{\exp(\mathcal{L}/2) - 1}. \tag{19}$$

Remark 6. The skew-symmetry between the evolution equations for kink and anti-kink, reflects the broken mirror symmetry $x \to -x$ of the cCH equation.

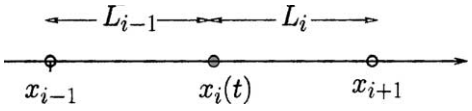

Fig. 4. Here $x_i(t)$ denotes the location of the ith phase boundary, $L_i(t) := x_{i+1} - x_i$ is the distance between the ith and $i+1$th phase boundary, and ● and ○ denote kink and anti-kink, respectively; given our indexing convention, i in this figure is understood to be odd.

In turn, when considering the evolution of distances between a neighboring kink/anti-kink pair, one observes two types of intervals; depending on the sign of the order parameter q in the given interval. Noting that $\dot{L}_i = \dot{x}_{i+1} - \dot{x}_i$, it follows from (18) that

$$\frac{\mathrm{d}L_i}{\mathrm{d}t} = (-1)^i [J(L_{i+1}) - J(L_{i-1})]. \tag{20}$$

4.2. $\mathcal{CDS}$ and scaling laws

The outcome of encounters between kinks and anti-kinks is readily visualized via the faceted-crystal application. First, if a pair meet, they annihilate since the interpolating facet disappears. Now in the case of coalescence of higher order, e.g. the ternary collision, a *parity law* arises. Namely, even groupings annihilate, and odd groupings result in the appearance of the dominant type. So, for example, in the case of two kinks colliding with a single anti-kink, we obtain a kink.

Definition 7 ($\mathcal{CDS}$). We refer to the coarsening dynamical system that arises from the evolution of (18), subject to the *parity* coarsening law outlined in the preceding paragraph, as $\mathcal{CDS}$.

The average separation between neighboring defects, namely the *morphological* length scale $\mathcal{L}_{\mathcal{M}}(t)$, grows as $\mathcal{CDS}$ evolves due to coalescence of kinks and anti-kinks. Now, previous large-scale simulations of $\mathcal{CDS}$ have been carried out in Emmot and Bray [13] for the specific choice $J(L) = 1/L$. They found that $\mathcal{L}_{\mathcal{M}} \sim t^{1/2}$, and also that the distribution function $P(L, t)$ (the fraction of domains which have size L at time t) scales in a self-similar manner; i.e.

$$P(L, t) = \frac{1}{\mathcal{L}_{\mathcal{M}}(t)} \hat{P}\left(\frac{L}{\mathcal{L}_{\mathcal{M}}(t)}\right)$$

for some numerically determined function $\hat{P}$. They noted furthermore, that this self-similar scaling of $P(L, t)$ occurred even for "early times"; in distinction with standard equilibrium phase separation where self-similar scaling occurs at "late times" only.

In our theory, the scaling law $\mathcal{L}_{\mathcal{M}}(t) \sim t^{1/2}$, which arises in the regime $\varepsilon \ll \mathcal{L}_{\mathcal{M}} \ll 1$, may be understood by the following simple scaling argument. First, we note that the flux function $J(L)$, Eq. (19), has the asymptotic form:

$$J(L) \sim \frac{1}{L} \quad \text{as} \quad L \to 0^+. \tag{21}$$

It follows, in the regime $\varepsilon \ll \mathcal{L}_{\mathcal{M}} \ll 1$, that (20) is (asymptotically) invariant with respect to the scaling

$$t \to \lambda^2 t, \qquad L \to \lambda L. \tag{22}$$

Hence, if we assume that the distribution function $P(L, t)$ scales in a self-similar manner, it follows that

$$\mathcal{L}_{\mathcal{M}}(t) \sim t^{1/2} \quad \text{for} \quad \varepsilon \ll \mathcal{L}_{\mathcal{M}} \ll 1.$$

5. Numerical simulations of $\mathcal{CDS}$ and cCH

In order to better understand the *coarsening pathway* of $\mathcal{CDS}$, a numerical simulation has been written using Mathematica. The problem of n kink/anti-kink pairs on a line of length L with periodic boundary conditions is

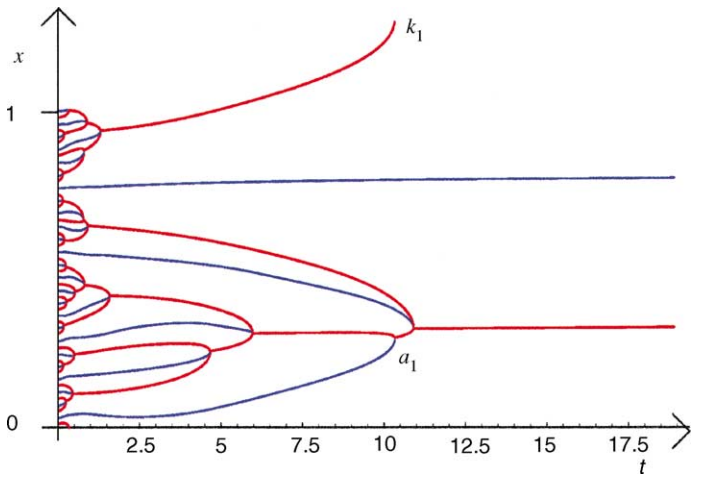

Fig. 5. Numerical simulation of $\mathcal{CDS}$ on domain of length 1 with periodic boundary conditions and $\varepsilon = 0.005$. The kink trajectories are marked in red and the anti-kink trajectories in blue. Note that the kink marked k_1 coalesces with the anti-kink marked a_1 due to the periodicity of the boundary conditions.

treated for $\varepsilon \ll 1$. For initial conditions in $\mathcal{CDS}$, we take an evenly spaced array of defects (kink alternating with anti-kink) with separation $d := L/2n$, and then perturb each location by a random distance taken from a normal distribution centered at 0 with covariance $d/20$. Coalescence of defects is identified when the distance between them comes within the prescribed tolerance, $\varepsilon/10$.

We present in Fig. 5 the result of our such a simulation of $\mathcal{CDS}$ for 25 kink/anti-kink pairs placed on a domain of unit length with $\varepsilon = 0.005$. One notes that there are no binary events. Furthermore, we see that the sole coarsening event is a specific ternary coalescence; two kinks coalesce with an anti-kink resulting in a kink. Larger-scale simulations (not presented here) also display a marked degree of self-similarity during coarsening. Finally, the coarsening stops at the appearance of a single kink/anti-kink pair, which subsequently preserves a fixed separation.

To validate the unusual coarsening features exhibited by $\mathcal{CDS}$, a direct numerical simulation of cCH with $\varepsilon = 0.1$ was carried out by Prof. A.A. Golovin; a pseudo-spectral explicit in time method on a periodic domain. The initial condition involved a small random (Gaussian) perturbation of the unstable homogeneous state $q = 0$. The simulation results are presented in Fig. 6, where the plotted length scale is the inner scale $X = x/\varepsilon$, and the time scale t has been re-scaled to $t \to t/\varepsilon^2$; note that the in the inner scale, the interfacial layers have width 1. One initially observes spinodal decomposition with a wavelength consistent with the dominant linear instability of the system. An interfacial regime subsequently emerges, and coarsening then proceeds solely via *kink-ternaries* as predicted by $\mathcal{CDS}$.

6. $\mathcal{CDS}$ theory

We now present a theoretical study of $\mathcal{CDS}$ which explains the coarsening features that have been observed in the simulations.

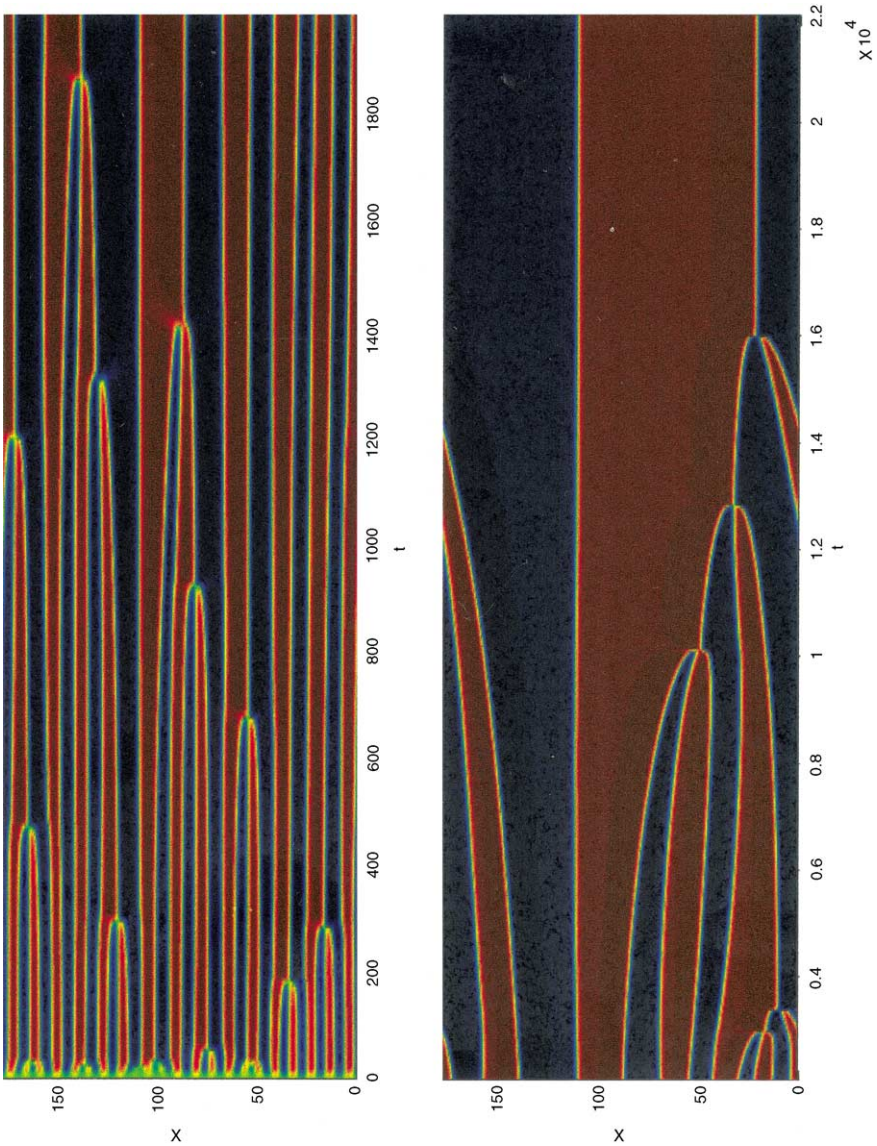

Fig. 6. Simulation of the cCH evolution equation for $\varepsilon = 0.1$, courtesy of A.A. Golovin. The color scheme is red for $q = 1$ through yellow, $q = 0$, to blue for $q = -1$. Note that the graphic is shown with respect to the *inner* length scale $X = x/\varepsilon$ and the re-scaled time $t \to t/\varepsilon^2$.

6.1. The "pinch instability"

First, we perform a linear stability analysis of (18) for an alternating array of equally spaced kink/anti-kinks on a periodic domain. We find that spectral properties are independent of domain size, and conclude that the dominant instability for the periodic domain (or unbounded line) involves a four-periodic "pinching"; two kinks "pinch" the intervening stationary anti-kink.

Let l_0 be the separation of an equally spaced alternating array of kink/anti-kinks on periodic domain of length $4nl_0$ ($n \in \mathbb{N}$). Linearizing the $4n$-dimensional dynamical system (18) about this state yields the $4n \times 4n$

matrix A:

$$A := -J'(l_0)\begin{bmatrix} 2 & -1 & 0 & & & \cdots & & & 0 & -1 \\ 1 & -2 & 1 & 0 & & \cdots & & & & 0 \\ 0 & -1 & 2 & -1 & 0 & \cdots & & & & 0 \\ 0 & & 1 & -2 & 1 & 0 & & & & 0 \\ & & & & \cdot & \cdot & \cdot & & & \\ & & & & \cdot & \cdot & \cdot & & & \\ 0 & & & & & \cdots & 0 & -1 & 2 & -1 \\ 1 & 0 & & & & \cdots & & 0 & 1 & -2 \end{bmatrix},$$

whose eigenvalues determine the instability of the uniform state. Notice that each successive row is a simple cyclic permutation of the previous row followed by multiplication by -1, and also that $-J'(l_0) > 0$.

We now present a characterization of the eigenvalues and eigenvectors of A in terms of the complex $4n$th roots of unity:

$$r_j := \mathrm{e}^{\mathrm{i}(\pi/2n)j}, \quad \text{where} \quad j = 0, 1, \ldots, 4n-1.$$

First, for each $j = 0, 1, \ldots$, we define the kth component of the vectors $\mathbf{u}^{(j)}, \mathbf{v}^{(j)} \in \mathbb{C}^{4n}$ as follows:

$$\mathbf{u}_k^{(j)} = (r_j)^k, \qquad \mathbf{v}_k^{(j)} = (-r_j)^k, \quad k = 1, \ldots, 4n.$$

We claim for each $j = 1, \ldots, 2n-1$, that the vectors $\mathbf{e}_j^+, \mathbf{e}_j^-$ given by

$$\mathbf{e}_j^+ := \left[1 + \cos\left(\frac{j\pi}{2n}\right)\right]^{1/2} \mathbf{u}_j + \left[1 - \cos\left(\frac{j\pi}{2n}\right)\right]^{1/2} \mathbf{v}_j,$$

$$\mathbf{e}_j^- := \left[1 + \cos\left(\frac{j\pi}{2n}\right)\right]^{1/2} \mathbf{u}_j - \left[1 - \cos\left(\frac{j\pi}{2n}\right)\right]^{1/2} \mathbf{v}_j$$

are eigenvectors of A with associated eigenvalues λ_j and $-\lambda_j$, respectively, where

$$\lambda_j = 2\sin\left(\frac{j\pi}{2n}\right).$$

This follows from a general theorem on *alternating circulant matrices* [24], motivated by this work, and which is related to the spectral properties of circulant matrices; see, e.g. [25]. Furthermore, the vectors $\mathbf{u}_0, \mathbf{v}_0$ are generalized eigenvectors of A with eigenvalue 0, and the set of vectors

$$\{\mathbf{u}_0, \mathbf{v}_0, \mathbf{e}_1^+, \ldots, \mathbf{e}_{2n-1}^+, \mathbf{e}_1^-, \ldots, \mathbf{e}_{2n-1}^-\}$$

constitute a basis for $\mathbb{C}^{4n}$.

The largest (positive) eigenvalue of 2 is attained when $j = n$, and the associated eigenvector is the four-periodic vector:

$$\mathbf{d} = [1, 0, -1, 0, \ldots]. \tag{23}$$

We note that in this most unstable direction the anti-kinks remain fixed and the kinks are "pinched" pairwise. Also, the structure of this unstable mode is independent of n; i.e. of the length of the periodic domain. Hence, we conclude that this is the most unstable mode for the unbounded line as well.

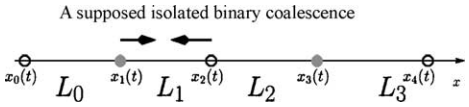

Fig. 7. Sketch of the impossible binary coalescence. Here, L_1 denotes the separation of the assumed coalescing pair, while L_0, L_2 and L_3 denote the separations of neighboring pairs. ● and ○ denote kink and anti-kink, respectively.

6.2. *The impossible binary and the unique kink-ternary*

Here we present an analysis of the dynamics of $\mathcal{CDS}$ in the fully nonlinear regime. We prove that isolated binary coalescence of phase boundaries is impossible, and furthermore that only one type of ternary event is permitted (two kinks meet an anti-kink), which we refer to as the *kink-ternary* since it results in a kink. These theoretical predictions are vividly confirmed in Figs. 5 and 6 which relate to numerical simulations of $\mathcal{CDS}$ and cCH, respectively. This behavior stands in marked contrast with the well-established prevalence of binary coalescence for the Cahn-Hilliard equation.

Theorem 8 (The impossible binary). *Isolated binary coalescence events are impossible for* $\mathcal{CDS}$.

Proof. We proceed by contradiction and suppose there exists a kink, $x_1(t)$, which coalesces at time T with an anti-kink, $x_2(t)$, while the neighbors remain separated throughout a preceding time interval (see Fig. 7); without loss of generality we have supposed the kink to be to the left of the anti-kink, and for convenience have re-indexed. So we have

$$\lim_{t\to T^-} L_1(t) = 0 \tag{24}$$

and

$$L_0(t), L_2(t), L_3(t) \geq d > 0 \quad \text{for all} \quad t \in (T-\delta, T] \tag{25}$$

for some $d > 0$ and some $\delta > 0$. Now from (20) and (25) we conclude that on the time interval $(T-\delta, T]$:

$$\frac{\mathrm{d}L_1}{\mathrm{d}t} = b_1(t), \tag{26}$$

$$\frac{\mathrm{d}L_2}{\mathrm{d}t} = -J(L_1) + b_2(t), \tag{27}$$

where the functions $b_1(t) := J(L_0(t)) - J(L_2(t))$ and $b_2(t) := J(L_3(t))$ are necessarily bounded due to assumption (25), i.e.

$$\max_{t\in(T-\delta,T]} |b_1(t)| = M_1 < \infty \quad \text{and} \quad \max_{t\in(T-\delta,T]} |b_2(t)| = M_2 < \infty. \tag{28}$$

Now (24), (26) and (28) imply

$$L_1(t) \leq M_1(T-t), \quad t \in (T-\delta, T], \tag{29}$$

Noting that $J(L)$ is monotone decreasing in L, while recalling (21), we deduce from (27)–(29) that

$$\frac{\mathrm{d}L_2}{\mathrm{d}t} \leq -\frac{1}{M_1(T-t)} + M_2 + \mathrm{O}(1) \quad \text{as} \quad t \to T^-. \tag{30}$$

But since $1/(T-t)$ is not integrable at T, we deduce from (30) that there exists a time $\tau \in (T-\delta, T)$ such that $L_2(\tau) = 0$. This contradicts (25), thereby establishing the theorem. □

Theorem 9 (*The kink-ternary*). *The coalescence of two kinks with an anti-kink is the only possible ternary coarsening event for $\mathcal{CDS}$.*

Proof. We proceed by contradiction. Suppose that two anti-kinks, $x_2(t)$ and $x_4(t)$, coalesce with the intervening kink, $x_3(t)$, at time T, while the neighboring kinks $x_1(t)$ and $x_5(t)$ remain at some finite distance. Proceeding as before, we have

$$\text{(i)} \quad \lim_{t\to T^-} L_2(t) = 0, \qquad \text{(ii)} \quad \lim_{t\to T^-} L_3(t) = 0, \tag{31}$$

while in some preceding time interval $[T-\delta, T]$, $\delta > 0$,

$$\frac{\mathrm{d}L_2}{\mathrm{d}t} = J(L_3) + b_1(t), \tag{32}$$

where the function $b_1(t) := -J(L_1(t))$ is bounded:

$$\max_{t\in(T-\delta,T]} |b_1(t)| = M_1 < \infty. \tag{33}$$

But, since $\lim_{L\to 0^+} J(L) = \infty$, it follows from part (ii) of (31) and (33) applied to (32) that there exists a time $\tau \in (T-\delta, T)$ for which

$$\frac{\mathrm{d}L_2}{\mathrm{d}t} > 0 \quad \text{for all} \quad t \in [\tau, T].$$

This contradicts part (i) of (31) and concludes the proof. □

Note that the preclusion of binary coalescence hinges on the non-integrability of the flux $J(L)$ at $L = 0$. Whereas, the exclusion of the two anti-kinks meeting a kink requires only that $J(L) \to \infty$ as $L \to 0^+$. Conversely, one may show that these conditions are also necessary for the associated properties to emerge. However, we also claim that though binary coalescence is not theoretically precluded for an integrable choice for J in $\mathcal{CDS}$ (e.g. $J(L) = 1/L^q$, with $0 < q < 1$), the generic coarsening event will still be an "approximate kink-ternary"; two kinks converging on an anti-kink, with one kink possibly annihilating the anti-kink "just before" the other arrives.

Remark 10 (The kink-ternary structure). The generic kink-ternary coarsening event displays a parabolic local structure in the shape of the paths of the coalescing kinks. Specifically, letting $L_1(t)$, $L_2(t)$ denote the separation of the two coalescing kinks from the intervening anti-kink, one may show that

$$L_1(t) = \sqrt[4]{2}\varepsilon^{1/2}(T-t)^{1/2} + \mathrm{o}((T-t)^{1/2}) = L_2(t) \quad \text{as} \quad t \to T^-,$$

where T is the coalescence time.

7. Analytical coarsening law for $\mathcal{CDS}$

We introduce here a *coarsening ansatz* for $\mathcal{CDS}$. It is based on several working hypotheses:

- Anti-kinks repel one another, as evidenced by the impossibility of the ternary event involving two anti-kinks meeting a kink. We assume that this repulsive interaction yields an "effectively periodic" structure to the coarsening system.
- The *pinch* instability identified for the idealized periodic array is the dominant mode for coarsening.

- The length scale distribution, $P(L, t)$, is self-similar throughout the coarsening process; we recall here that Emmott and Bray numerically observed self-similarity even at "early times" [13].
- A scale-invariant perturbation of a periodic array faithfully models the coupling of "effective periodicity" with the scale-invariance of $P(L, t)$ in the coarsening process.

Based on this ansatz, we deduce a theoretical coarsening law for the average length scale as a function of time. It stands in excellent agreement with results obtained from direct simulation of cCH [14]. A precise description follows.

7.1. The coarsening ansatz

An equally spaced array of kink/anti-kinks on a domain $\mathcal{I}$ (periodic or unbounded) is an unstable critical point for the dynamical system (18). Motivated by the linear stability analysis of Section 6.1, we study the initial-value problem associated with a scale-invariant disturbance η of this state in the direction of the most unstable eigenvector, Eq. (23), **d**. Specifically, we fix the location of the anti-kinks while pairwise pinching the kinks together by a scale-invariant distance ηl_0, where l_0 is the initial separation and $\eta > 0$ is a small dimensionless constant; see Fig. 8.

It follows from the symmetry of the initial data that the solution is a periodic extension of the elementary initial-value problem involving two pairs of kinks and anti-kinks on a periodic domain of length $4l_0$, subject to the dynamics given by (18); this reduced initial-value problem is illustrated in Fig. 9. One sees that the anti-kinks will remain fixed as the solution evolves, while the two kinks move towards the initially closer anti-kink (here, the upper one). They subsequently coalesce at the (upper) anti-kink, leaving a kink, in a finite time T characterized by the simple target-time problem:

$$\frac{\mathrm{d}s}{\mathrm{d}t} = [J(l_0 - s) - J(l_0 + s)], \qquad s(0) = \eta l_0, \qquad \lim_{t \to T^-} s(t) = l_0. \tag{34}$$

Referring to Fig. 8, we see that the an initial morphological length scale l_0 will be doubled in the *doubling time* T.

We may explicitly calculate the doubling time T of (34), as a function of the initial length l_0 and perturbation constant η, upon recalling (19):

$$\begin{aligned} T = \hat{T}(l_0, \eta) &= \int_{\eta l_0}^{l_0} \frac{\mathrm{d}s}{J(l_0 - s) - J(l_0 + s)} \\ &= \frac{4\sqrt{2}}{\varepsilon} \left[(\mathrm{e}^{l_0/2} + \mathrm{e}^{-l_0/2})[\operatorname{arctanh}(\mathrm{e}^{-\eta l_0/2}) - \operatorname{arctanh}(\mathrm{e}^{-l_0/2})] + (1 - \eta)\frac{l_0}{2} + \ln\left(\frac{\mathrm{e}^{\eta l_0} - 1}{\mathrm{e}^{l_0} - 1}\right)\right]. \end{aligned} \tag{35}$$

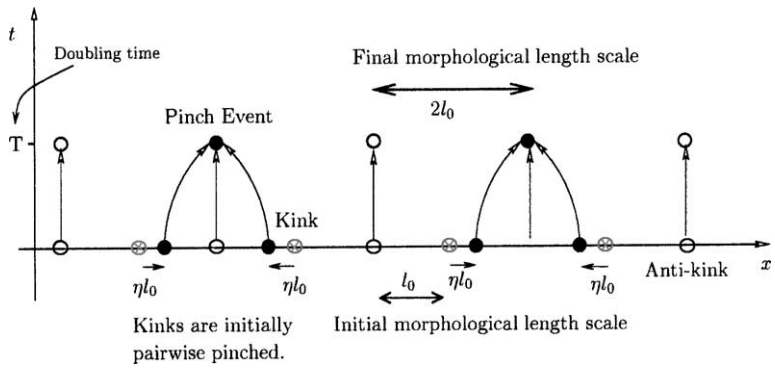

Fig. 8. The length scale doubling ansatz: ● and ○ denote the kink and anti-kink, while ⊗ denotes the location of the kink prior to the small offset perturbation in the most unstable direction η**d**; recall Eq. (23). The subsequent temporal evolution of kinks and anti-kinks locations is marked with arrows, concluding with *kink-ternary* coarsening events at time T.

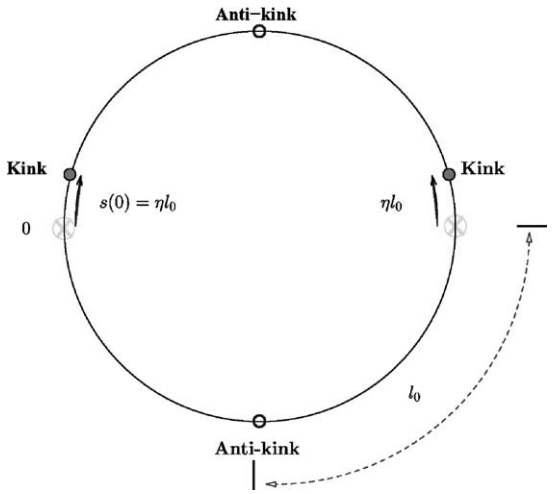

Fig. 9. The elementary period-doubling pinch event: ● and ○ denote the kink and anti-kink, while ⊗ denotes the location of the kink prior to the small offset perturbation in the most unstable direction $\eta\mathbf{d}$; recall Eq. (23).

Remark 11. We view the dimensionless parameter η as measuring the deviation of lengths in the coarsening structure from the mean length. Our ansatz implicitly assumes that the distribution of lengths around the mean is scale-invariant throughout the coarsening. One may choose to go beyond self-similarity and assume a dependence of η on the length scale l.

7.2. Theoretical coarsening law

Assuming self similarity in the coarsening process, we may iterate this period-doubling ansatz. This yields a geometric increase in the length scale in a known time period. Idealizing the initial length scale to be infinitesimally small relative to the observed length scales, we deduce the following (implicit) theoretical coarsening law for the morphological length scale $\mathcal{L}_\mathcal{M}$ as a function of time t:

$$t = \sum_{i=1}^{i=\infty} \hat{T}\left(\frac{\mathcal{L}_\mathcal{M}}{2^i}, \eta\right). \tag{36}$$

A numerical log–log plot of this theoretical scaling law is shown (with re-scaled time) in Fig. 10 for the choice $\eta = 0.001$. It displays the scaling $\mathcal{L}_\mathcal{M}(t) \sim t^{1/2}$, expected from the earlier self-similar scaling analysis of Section 4.2 in the regime $\varepsilon \ll \mathcal{L}_\mathcal{M} \ll 1$. A crossover regime, in which the coarsening rate slows, emerges when the (dimensionless) morphological length scale $\mathcal{L}_\mathcal{M} \sim 1$. Recalling (4), we understand that this crossover occurs at the Peclet length scale, where convection is balancing diffusion. Finally, the coarsening becomes logarithmically slow as $\mathcal{L}_\mathcal{M} \to \infty$, consistent with the convergence of the cCH to CH in this limit.

Since our *pinch ansatz* involves a description of the *coarsening path*, we are also able to identify the scaling constant associated with the $t^{1/2}$ coarsening regime. First, the doubling time (35) has the asymptotic form:

$$\hat{T}(l_0, \eta) = \frac{1}{2\sqrt{2}\varepsilon}(\eta^2 - 2\ln\eta - 1)l_0^2 \quad \text{as} \quad l_0 \to 0^+.$$

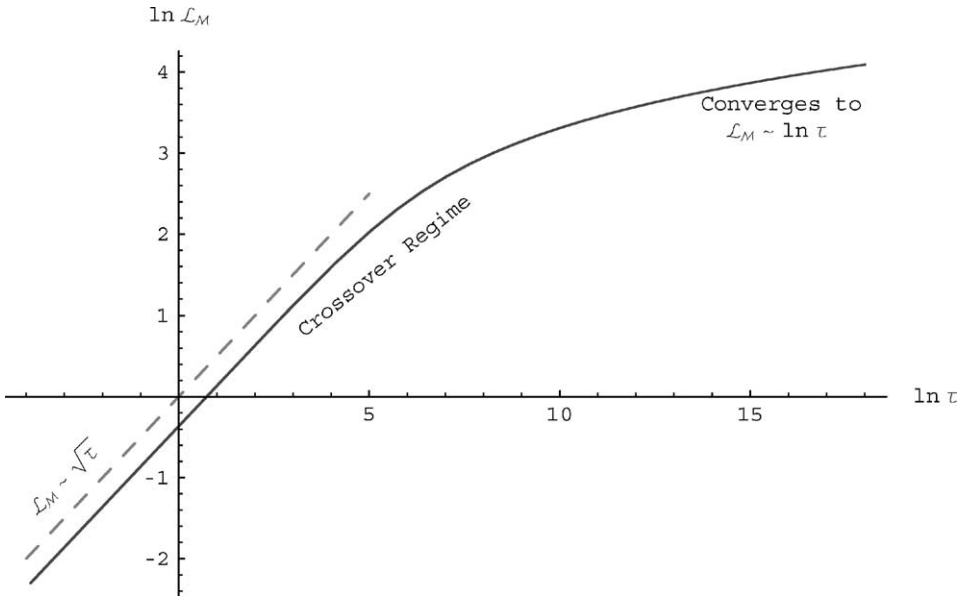

Fig. 10. Numerical plot of the theoretical scaling law (36) exhibiting the scaling of the morphological length $\mathcal{L}_M$ versus the re-scaled *slow time* $\tau := \varepsilon t$ for the choice of *disturbance parameter* $\eta = 0.001$. Note that crossover scaling arises when the dimensionless morphological length scale $\mathcal{L}_M \sim \mathrm{O}(1)$; i.e. at the Peclet length scale $\mathcal{L}_\mathcal{P}$ (4).

Hence, the theoretical scaling law (36) yields

$$\mathcal{L}_M = \frac{\sqrt{3}}{\sqrt[4]{2}(\eta^2 - 2\ln\eta - 1)^{1/2}} \varepsilon^{1/2} t^{1/2} \quad \text{as} \quad \mathcal{L}_M \to 0^+. \tag{37}$$

Note that the scaling pre-factor of $t^{1/2}$ appearing in (37), $c(\eta)$, is monotone increasing in the interval $\eta \in (0, 1)$, and furthermore

$$\lim_{\eta \to 0^+} c(\eta) = 0 \quad \text{and} \quad \lim_{\eta \to 1^-} c(\eta) = \infty.$$

One may thus envision determining η from a numerical simulation of either cCH or $\mathcal{CDS}$, by identifying the scaling constant associated with the $t^{1/2}$ coarsening regime.

8. Conclusions

We have considered the coarsening dynamics of a convective Cahn-Hilliard equation (cCH) in one space dimension. A sharp-interface theory for the evolution of *phase boundaries* is derived through a matched asymptotic expansion arising when the phase boundary width $\varepsilon \to 0^+$. Due to convection, two non-symmetrically related phase boundaries emerge (kink and anti-kink), which then interact to leading order through a convection–diffusion flux of the order parameter. This yields a dynamical system ($\mathcal{CDS}$) for kink/anti-kink locations, which coarsens in time through their coalescence. Our theory is valid for all morphological (characteristic) length scales $\mathcal{L}_M \gg \varepsilon$; i.e. whenever the system enters the *interfacial regime*. Novel coarsening properties of $\mathcal{CDS}$ have been identified; binary coalescence is impossible, and there is a unique ternary coalescence (*the kink-ternary*). Furthermore, $\mathcal{CDS}$ predicts the temporal scaling law $\mathcal{L}_M \sim t^{1/2}$, provided $\varepsilon \ll \mathcal{L}_M \ll 1$. All of the above have been confirmed by direct numerical simulations on cCH and $\mathcal{CDS}$.

A *pinching mechanism* has been identified as the dominant linear instability of an alternating periodic array of kink/anti-kinks. A self-similar period-doubling ansatz, involving a scale-invariant recursion of the elementary pinching mechanism, is subsequently proposed as a description of the entire coarsening path. This yields, in turn, a theoretical coarsening law for the morphological length scale $\mathcal{L}_{\mathcal{M}}$ as a function of time t. It stands in good qualitative agreement with both the direct computations $\mathcal{CDS}$, and also the numerical simulations of cCH [14].

The coarsening dynamical system approach developed here offers a flexible framework for the identification of coarsening laws in 1D systems where localized structures (defects) interact. It embodies the principle that the evolution of structure is essentially determined by the local structure of the defects and their mutual interaction.

Acknowledgements

SJW was supported by the Max-Planck-Institute for Mathematics in the Sciences (MIS), Leipzig in the initial stages of this project and later by the NSF N.I.R.T. grant #DMR-0102794. SHD was supported by the NSF N.I.R.T. grant #DMR-0102794. The authors would like to thank Prof. A.A. Golovin for kindly providing numerical simulations of the cCH equation to validate the *kink-ternary* prediction of our theory.

Appendix A. Matched asymptotic analysis

The governing equation (5) is singularly perturbed in the limit $\varepsilon \to 0^+$, and so is referred to as the outer equation. In this section, we perform the associated matched asymptotic expansions. Since the parameter ε sets a length scale for transitions, we shall see that the associated outer problem yields a sharp-interface theory.

We assume the asymptotic expansion of (5) takes the form:

$$q = q_0(x) + q_1(x)\varepsilon + \cdots \quad \text{(outer expansion)}, \qquad k(t,\epsilon) = k_0(t) + k_1(t)\varepsilon + \cdots \quad \text{(kink expansion)},$$
$$a(t,\epsilon) = a_0(t) + a_1(t)\varepsilon + \cdots \quad \text{(anti-kink expansion)}.$$

The inner equation arises from re-scaling to the inner length scale ε (in units $\mathcal{L}_P$). Since the kinks $k(t;\varepsilon)$ and anti-kinks $a(t;\varepsilon)$ are in general moving, we need to select an inner coordinate with respect to a moving frame. So, for the kink at $x = k^i(t;\varepsilon)$, we take the inner coordinate X to be

$$X = \frac{x - k(t;\varepsilon)}{\varepsilon}$$

and re-write (5) in terms of the inner solution $Q(X,t) = q(x,t)$ as

$$\varepsilon^2 Q_t - \varepsilon \dot{k}(t;\varepsilon) Q_X - \varepsilon Q Q_X = (Q^3 - Q - Q_{XX})_{XX}. \tag{A.1}$$

We proceed in a similar fashion for the anti-kink $a(t)$.

Now q satisfies the conservation law

$$q_t + J_x = 0,$$

where

$$J = -\hat{W}'(q)_x + \tfrac{1}{2}\varepsilon q^2 + \varepsilon^2 q_{xxx}. \tag{A.2}$$

Hence, across the kinks and anti-kinks we have the Rankine-Hugoniot relation:

$$\dot{k}(t)[q]_{k(t;\varepsilon)} = [J]_{k(t;\varepsilon)}, \tag{A.3}$$

where $[J]_{k(t;\varepsilon)}$ and $[q]_{k(t;\varepsilon)}$ denote, respectively, the jump in the flux J and the order parameter q across the kink at $x = k(t;\varepsilon)$; similarly for the anti-kink.

Before proceeding with the matching, we convert the free boundary-value problem associated with the outer solution to a fixed domain by introducing the following coordinate transformation. Assume that the initial distribution of kink and anti-kink locations is given by k^i, $a^i \in \mathbb{R}$ ($i \in \mathbb{Z}$), where

$$k^i < a^i < k^{i+1} \quad \forall\, i \in \mathbb{Z}.$$

We define $\Psi : \mathbb{R} \times [O, T) \times [0, \bar{\varepsilon}) \to \mathbb{R}$, through

$$\Psi(y,t,\varepsilon) := \begin{cases} k_i(t,\varepsilon) + \dfrac{a_i(t,\varepsilon) - k_i(t,\varepsilon)}{a^i - k^i}(y - k^i), & x \in (k^i, a^i), \\ a_{i-1}(t,\varepsilon) + \dfrac{k_i(t,\varepsilon) - a_{i-1}(t,\varepsilon)}{k^i - a_{i-1}}(y - a_{i-1}), & x \in (a_{i-1}, k^i). \end{cases}$$

Now we introduce the velocity field $\mathcal{V}(y,t;\varepsilon) := \Psi_t(y,t,\varepsilon)$:

$$\mathcal{V}(y,t;\varepsilon) = \begin{cases} \dot{k}_i(t,\varepsilon) + \dfrac{\dot{a}_i(t,\varepsilon) - \dot{k}_i(t,\varepsilon)}{a^i - k^i}(y - k^i), & x \in (k^i, a^i), \\ \dot{a}_{i-1}(t,\varepsilon) + \dfrac{\dot{k}_i(t,\varepsilon) - \dot{a}_{i-1}(t,\varepsilon)}{k^i - a_{i-1}}(y - a_{i-1}), & x \in (a_{i-1}k^i), \end{cases}$$

and the piecewise constant (in y) stretch function $\mathcal{S}(y,t;\varepsilon)$:

$$\mathcal{S}(y,t;\varepsilon) := \frac{1}{\partial\Psi/\partial y} = \begin{cases} \dfrac{a^i - k^i}{a_i(t,\varepsilon) - k_i(t,\varepsilon)}, & y \in (k^i, a^i), \\ \dfrac{k^i - a_{i-1}}{k_i(t,\varepsilon) - a_{i-1}(t,\varepsilon)}, & y \in (k^i, a_{i-1}). \end{cases}$$

The outer equation (5) then takes the form:

$$q_t - \mathcal{V}q_y - \mathcal{S}qq_y = \mathcal{S}^2[\hat{W}'(q) - \varepsilon^2\mathcal{S}^2 q_{yy}]_{yy} \tag{A.4}$$

on each open interval (k^i, a^i) and (a^i, k^{i+1}).

A.1. Asymptotic match to O(1)

Setting $\varepsilon = 0$ we deduce from (A.1) that the inner solution has the form:

$$\mathcal{Q}_0(X) := \tanh X \tag{A.5}$$

about the kink $k(t;\varepsilon)$, and similarly, across the anti-kink $a(t;\varepsilon)$ we deduce

$$\mathcal{Q}_0(X) := -\tanh X. \tag{A.6}$$

We now match the leading-order inner solutions (A.5) and (A.6) to the outer solution. Taking first a kink/anti-kink interval (k^i, a^i) and matching to order O(1) we deduce, from (A.4)–(A.6), the following boundary-value problem:

$$(q_0)_t - \frac{a_0^i(t) - k_0^i(t)}{a^i - k^i} q_0 (q_0)_y = \left(\frac{a_0^i(t) - k_0^i(t)}{a^i - k^i}\right)^2 [(q_0)^3 - q_0]_{yy}, \qquad q_0[k^i, t] = 1 = q_0[a^i, t],$$

from which we conclude that

$$q_0(y,t) \equiv 1 \quad \text{for} \quad y \in (k^i, a^i). \tag{A.7}$$

We deduce in a similar manner that

$$q_0(y,t) \equiv -1 \quad \text{for} \quad y \in (a^i, k^{i+1}). \tag{A.8}$$

Noting (A.2), (A.7) and (A.8), it follows from the Rankine-Hugoniot relation (A.3) that

$$\dot{k}_0^i(t) = 0 \quad \text{and} \quad \dot{a}_0^i(t) = 0. \tag{A.9}$$

A.2. Asymptotic match to O(ε)

From (A.9), we see that the kink and anti-kink velocities are of order $\mathrm{O}(\varepsilon)$ and therefore (A.1) is asymptotically equivalent through order $\mathrm{O}(\varepsilon)$ with the time-independent equation:

$$-\varepsilon Q Q_X = (Q^3 - Q - Q_{XX})_{XX}. \tag{A.10}$$

Now (7) has two exact solutions $\mathcal{K}(X)$ and $\mathcal{A}(X)$ given by

$$\mathcal{K}(X) := \left(1 + \frac{\varepsilon}{\sqrt{2}}\right)^{1/2} \tanh\left[\left(1 + \frac{\varepsilon}{\sqrt{2}}\right)^{1/2} X\right] \quad \text{(kink)}$$

and

$$\mathcal{A}(X) := -\left(1 - \frac{\varepsilon}{\sqrt{2}}\right)^{1/2} \tanh\left[\left(1 - \frac{\varepsilon}{\sqrt{2}}\right)^{1/2} X\right] \quad \text{(anti-kink)}$$

which will be matched to the outer solution. We note here that the asymptotic values as $X \to \infty$ of $\mathcal{K}(X)$ and $\mathcal{A}(X)$ are

$$\lim_{X \to \pm\infty} \mathcal{K}(X) = \pm\left(1 + \frac{\varepsilon}{\sqrt{2}}\right)^{1/2}, \tag{A.11}$$

$$\lim_{X \to \pm\infty} \mathcal{A}(X) = \mp\left(1 - \frac{\varepsilon}{\sqrt{2}}\right)^{1/2}. \tag{A.12}$$

Returning to (A.4), we note that $\mathcal{S} = 1 + \mathrm{O}(\varepsilon)$ since $\dot{k}(t;\varepsilon) = \mathrm{O}(\varepsilon) = \dot{a}(t;\varepsilon)$. So, it follows from (A.4), (A.7) and (A.8) and the $\mathrm{O}(\varepsilon)$ matching with (A.11) and (A.12) that q_1 satisfies the following boundary-value problem:

$$(q_1)_t - (q_1)_y = [2q_1]_{yy}, \qquad q_1(k^i, t) = \frac{1}{2\sqrt{2}} \quad \text{for} \quad q_1(a^i, t) = -\frac{1}{2\sqrt{2}}.$$

Also, proceeding in a similar manner for the anti-kink/kink interval (a^i, k^{i+1}), we arrive at the companion boundary-value problem:

$$(q_1)_t + (q_1)_x = [2q_1]_{xx}, \qquad q_1(a^i, t) = \frac{1}{2\sqrt{2}} \quad \text{for} \quad q_1(k^{i+1}, t) = -\frac{1}{2\sqrt{2}}.$$

We conclude that

$$q_1(y,t) = q_1(y) := \begin{cases} \dfrac{1}{2\sqrt{2}} - \dfrac{1}{\sqrt{2}} \dfrac{1 - \exp[-(y - k^i)/2]}{1 - \exp[-(a^i - k^i)/2]}, & k^i \le y \le a^i, \\ -\dfrac{1}{2\sqrt{2}} + \dfrac{1}{\sqrt{2}} \dfrac{1 - \exp[(y - k^{i+1})/2]}{1 - \exp[-(k^{i+1} - a^i)/2]}, & a^i \le y \le k^{i+1}. \end{cases} \tag{A.13}$$

Now expanding the Rankine-Hugoniot relation (A.3) in powers of ε, utilizing (A.2) and (A.13) and the O(1) conditions, yields upon matching the O(ε) terms:

$$\dot{k}_1^i(t) = \frac{1}{2\sqrt{2}}[\hat{f}(a^i - k^i) - \hat{f}(k^i - a^{i-1})] \tag{A.14}$$

and

$$\dot{a}_1^i(t) = \frac{1}{2\sqrt{2}}[\hat{f}(a^i - k^i) - \hat{f}(k^{i+1} - a^i)], \tag{A.15}$$

where

$$\hat{f}(l) := \frac{1}{e^{l/2} - 1}.$$

References

[1] A.J. Bray, Theory of phase ordering kinetics, Adv. Phys. 43 (3) (1997) 357–459.
[2] J.W. Cahn, J.E. Hilliard, Free energy of nonuniform systems. I. Interfacial free energy, J. Chem. Phys. 28 (1958) 258.
[3] J.W. Cahn, W.C. Carter, Crystal shapes and phase equilibria: a common mathematical basis, Metall. Mater. Trans. A 27 (6) (1996) 1431–1440.
[4] T. Kawakatsu, T. Munakata, Kink dynamics in a one-dimensional conserved TDGL system, Prog. Theor. Phys. 74 (1985) 11–19.
[5] J.W. Cahn, D.W. Hoffman, A vector thermodynamics for anisotropic surfaces. II. Curved and faceted surfaces, Acta Metall. 22 (1974) 1205.
[6] J. Stewart, N. Goldenfeld, Spinodal decomposition of a crystal surface, Phys. Rev. A 46 (1992) 6505.
[7] M. Siegert, Coarsening dynamics of crystalline thin films, Phys. Rev. Lett. 81 (25) (1998) 5481.
[8] A.A. Chernov, Stability of faceted faces, J. Cryst. Growth 24/25 (1974) 11.
[9] F. Liu, H. Metiu, Dynamics of phase-separation of crystal surfaces, Phys. Rev. B 48 (1993) 5808.
[10] D. Moldovan, L. Golubovic, Interfacial coarsening dynamics in epitaxial growth with slope selection, Phys. Rev. E 61 (6) (2000) 6190–6214.
[11] A.A. Golovin, S.H. Davis, A.A. Nepomnyashchy, A convective Cahn-Hilliard model for the formation of facets and corners in crystal growth, Physica D 118 (1998) 202–230.
[12] P. Smilauer, M Rost, J. Krug, Fast coarsening in unstable epitaxy with desorption, Phys. Rev. E 59 (6) (1999) 6263.
[13] C.L. Emmott, A.J. Bray, Coarsening dynamics of a one-dimensional driven Cahn-Hilliard system, Phys. Rev. E 54 (1996) 4568.
[14] A.A. Golovin, A.A. Nepomnyashchy, S.H. Davis, M.A. Zaks, Convective Cahn-Hilliard models: from coarsening to roughening, Phys. Rev. Lett. 86 (8) (2001) 1550–1553.
[15] K. Leung, Theory of morphological instability in driven systems, J. Stat. Phys. 61 (1990) 345.
[16] S.J. Watson, Crystal growth, coarsening and the convective Cahn-Hilliard equation, in: P. Colli, C. Verdi, A. Visintin (Eds.), Free Boundary Problems (Trento, 2002), Birkhauser, Basel, in press.
[17] S.J. Watson, Coarsening dynamics for the convective Cahn-Hilliard, Seminar: Interphase 2001, University of Maryland, January 9–12, 2002.
[18] S.J. Watson, F. Otto, B. Rubinstein, S.H. Davis, Coarsening dynamics for the convective Cahn-Hilliard equation, Preprint 35/2002, Max Planck Institute for Mathematics in the Sciences, Leipzig, April 2002. http://www.mis.mpg.de.
[19] A. Di Carlo, M.E. Gurtin, P. Podio-Guidugli, A regularised equation for anisotropic motion-by curvature, SIAM J. Math. Anal. 52 (1992) 1111–1119.
[20] M.E. Gurtin, Thermomechanics of Evolving Phase Boundaries in the Plane, Clarendon Press, Oxford, 1993.
[21] T. Willmore, Riemannian Geometry, Oxford University Press, New York, 1993.
[22] H. Calisto, M. Clerc, R. Rojas, E. Tirapegui, Bubbles interactions in the Cahn-Hilliard equation, Phys. Rev. Lett. 85 (18) (2000) 3805–3808.
[23] X. Sun, M.J. Ward, Dynamics and coarsening of interfaces for the viscous Cahn-Hilliard equation in one spatial dimension, Stud. Appl. Math. 105 (2000) 203–234.
[24] S.J. Watson, The spectrum and generalized eigenvector basis of alternating circulant matrices, submitted for publication.
[25] R. Bellman, Introduction to Matrix Analysis, McGraw-Hill, New York, 1970.